



Communication

Pre-Orientele Southwest Peak-Ring Basin: Gravity Structure, Geologic Characteristics, and Influence on Orientele Basin Ring Formation and Ejecta Emplacement

Jin Zhu Ji ^{1,2}, James W. Head ³ and Jianzhong Liu ^{2,4,*}¹ School of Mining, Inner Mongolia University of Technology, Hohhot 010051, China; jijin Zhu@imut.edu.cn² Center for Lunar and Planetary Sciences, Institute of Geochemistry, Chinese Academy of Sciences, Guiyang 550081, China³ Department of Earth, Environmental and Planetary Sciences, Brown University, Providence, RI 02912, USA; james_head@brown.edu⁴ Center for Excellence in Comparative Planetology, Chinese Academy of Sciences, Hefei 230026, China

* Correspondence: liujianzhong@mail.gyig.ac.cn

Abstract: The Orientele impact basin is the youngest and most well-preserved of the lunar multi-ring basins. The generally well-preserved ring structures and basin facies are distinctly anomalous in the southwestern quadrant; the outer Cordillera ring extends significantly outward, the Outer and Inner Rook mountain rings are more poorly developed and show anomalous characteristics, and the Montes Rook Formation varies widely from its characteristics elsewhere in the basin interior. Based on the gravity, image, and topography data, we confirmed that the southwest region of the Orientele basin represents the location of a pre-existing ~320 km rim–crest diameter peak–ring basin centered at 108.8°W, 28.4°S, and characterized by an ~170 km peak–ring diameter. We model the structure and morphology of this large pre-Orientele peak–ring basin (about one-third the diameter of Orientele) and show that its presence and negative relief had a distinctive influence on the development of the basin rings (disrupting the otherwise generally circular continuity and causing radial excursions in their locations) and the emplacement of ejecta (causing filling of the low region represented by the peak–ring basin, creating anomalous surface textures, and resulting in late stage ejecta movement in response to the pre-existing peak–ring basin topography. The location and preservation of the peak–ring basin Bouguer anomaly strongly suggest that the rim crest of the Orientele basin excavation cavity lies at or within the Outer Rook Mountain ring.

Keywords: pre-Orientele southwest peak–ring basin; topographic reconstruction; Orientele basin ring formation; ejecta emplacement



Citation: Ji, J.; Head, J.W.; Liu, J. Pre-Orientele Southwest Peak-Ring Basin: Gravity Structure, Geologic Characteristics, and Influence on Orientele Basin Ring Formation and Ejecta Emplacement. *Remote Sens.* **2021**, *13*, 2635. <https://doi.org/10.3390/rs13132635>

Academic Editor: Akira Iwasaki

Received: 6 May 2021

Accepted: 27 June 2021

Published: 5 July 2021

Publisher's Note: MDPI stays neutral with regard to jurisdictional claims in published maps and institutional affiliations.



Copyright: © 2021 by the authors. Licensee MDPI, Basel, Switzerland. This article is an open access article distributed under the terms and conditions of the Creative Commons Attribution (CC BY) license (<https://creativecommons.org/licenses/by/4.0/>).

1. Introduction

The Orientele basin is the youngest multi-ring basin and preserved the origin characteristics of the impact basin well [1–5] displaying four distinct concentric rings, Inner Depression (~320 km), Inner Rook ring (~480 km), Outer Rook ring (~620 km), and Cordillera ring (~930 km), respectively. Based on previous research results and topographical features, we have initially drawn different ring structures of the Orientele basin (Figure 1). The Cordillera ring is continuous and well-preserved in all directions around the basin except the southwestern region (Figure 1), where the massifs most extensively developed and ring structures are difficult to distinguish and several previous mapping efforts have noted an outward excursion of massifs and ring structures in this region [3,4,6,7]. Meanwhile, the Montes Rook Formation is largely restricted to the Orientele interior and the smooth member of the Montes Rook Formation is mainly concentrated in the southwestern quadrant of the basin interior with minor extensions beyond the Cordillera basin rim crest [7]. In addition, the Outer Rook ring is likewise distorted from its mostly circular expression in

this topographically complex southwestern region, displaying wider ring massifs. Why are the Cordillera and Outer Rook ring not as well defined in this location? The complicated structures have been suggested to be related to an oblique basin-forming impact, orientation of preexisting crustal weaknesses [6], the presence of a pre-Oriente basin [8–10], or increasing lithospheric thickness towards the west [11]. Head et al. (2010) recognized the southwestern region as a basin based on the Lunar Reconnaissance Orbiter (LRO)'s Lunar Orbiter Laser Altimeter (LOLA) data that superposed on a hillshade rendering of LOLA topography [12]. On the basis of GRAIL and LOLA data, Neumann et al. (2015) recognized this basin as a peak–ring basin with only one topographic ring and no interior peak–ring or central peak structure [13], but the diameter is only ~276 km, which is underestimated when compared to the Schrödinger basin (~325 km) with a similar Bouguer gravity anomaly pattern. Morse et al. (2018) pointed out the existence of several pre-existing impact structures measuring between 60 and 150 km in diameter which disrupted the coherent development of the Cordillera scarp [14]. However, these pre-Oriente Basin topographic features are still unknown, which raises some of the following questions: (1) How does pre-existing topography influence the nature, style, and formation of the rings of Oriente basin and what ring is the closest approximation to the transient cavity rim (excavation/ejection) boundary)? (2) What is the role of pre-existing topography in assisting/inhibiting/modifying ejecta emplacement of the Oriente basin?

The occurrence of a highly degraded pre-Oriente peak–ring basin (PRB) adjacent to the Oriente basin to the southwest could be an important key to address these questions. In this study, based on the GRAIL bouguer anomaly data, Wide Angle Camera (WAC) of Lunar Reconnaissance Orbiter Camera (LROC) data, and SLDEM2015 data (a topography product of the LOLA data with the SELENE Terrain Camera stereo data), we confirmed that a pre-Oriente Southwest PRB is located at the southwest region of Oriente basin. The center of this southwest PRB is 108.8°W, 28.4°S with a ~320 km rim–crest diameter and a ~170 km peak–ring diameter.

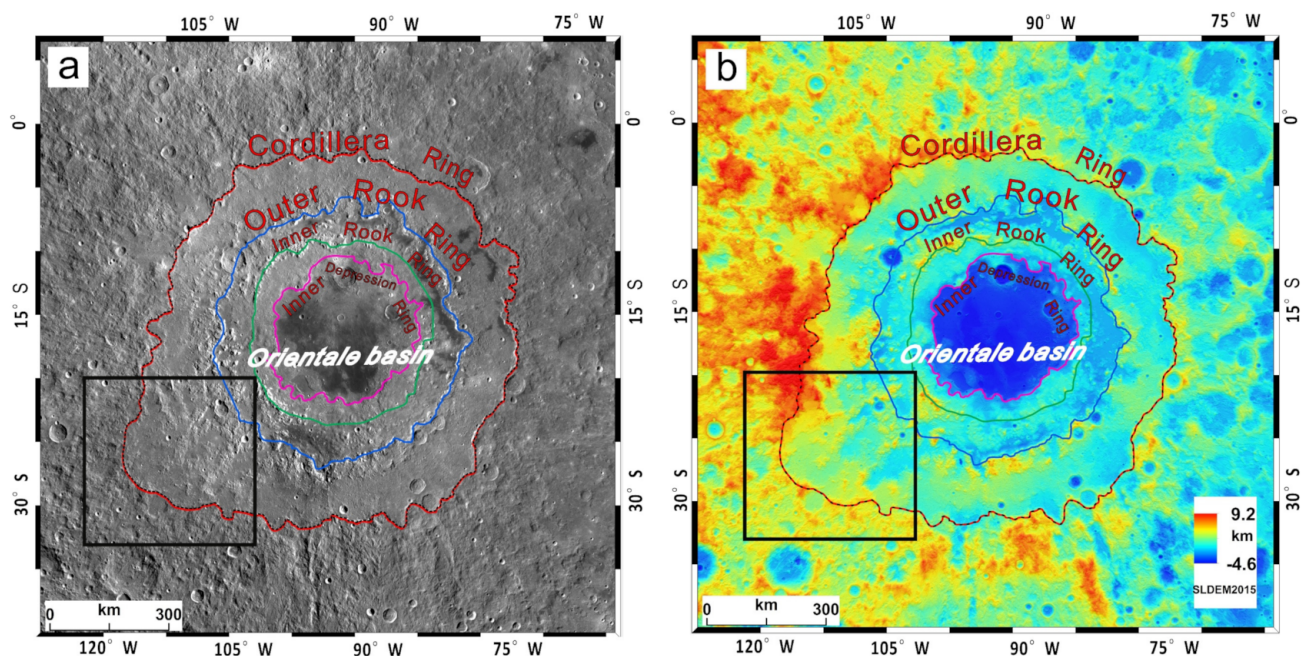


Figure 1. Ring configuration of the Oriente basin and black box is the study region: (a) WAC image mosaic; (b) SLDEM2015 colored gridded topography (orthographic projection centered at 19°S, 95°W).

2. Data and Methods

2.1. Data

The Lunar Reconnaissance Orbiter Camera (LROC) is a system of three cameras mounted on the Lunar Reconnaissance Orbiter (LRO) that capture high resolution black and white images and moderate resolution multi-spectral images of the lunar surface. WAC image mosaic has a spatial resolution of 100 meters/pixel in seven color bands over a 60 km swath [15]. The Gravity Recovery and Interior Laboratory (GRAIL) mission flies twin spacecraft in tandem orbits around the moon for several months to measure its gravity field in unprecedented detail [16,17]. The current gravity model, GRGM1200A, is derived from spherical harmonic expansions of the lunar gravitational potential to degree and order 1200, with sensitivity down to ~4.5 km resolution [18], archived at the PDS Geosciences node (<http://pds-geosciences.wustl.edu/>, accessed on 6 May 2021). Spacecraft are sensitive to the entire planetary gravity fields, also called “free-air”. Through geophysical modeling, such gravity field measurements can be used to understand the subsurface structure and density of planetary bodies. Assuming a constant crustal density, the gravity field induced by the topography is called Bouguer correction. The Bouguer gravity can be used to highlight the contributions from subsurface mass anomalies [16]. The SLDEM2015 digital elevation model (DEM) with a resolution of 512 pixels per degree (59 m/pixel) is the combination product of the LOLA data with the SELENE Terrain Camera stereo data [19] and available from the Planetary Data System LOLA data node (<http://imbrium.mit.edu/EXTRAS/SLDEM2015/>, accessed on 6 May 2021), which has many geophysical and cartographic applications in lunar science, as well as exploration and mission design.

2.2. Methods

In this study, for the Bouguer map, we truncated the Bouguer gravity data into 7–600 degree and order, aiming to highlight mid-to short-wavelength structure and reduce the effects of regional (long-wavelength) patterns on our analyses [20–22]. Firstly, we determined the center of this candidate PRB according to the maximum Bouguer gravity anomaly in the central area. In order to reduce the influence of local changes of gravity anomalies and obtain characteristics of the Bouguer gravity anomaly for this region more accurately, we have measured the azimuth radial profiles of Bouguer anomaly by 1° bearing from the north (clockwise, total 360 lines), and we computed the average radial profile to estimate the Bouguer gravity anomaly trend from the basin center to outward of PRB and determine the place of the minimum Bouguer gravity anomaly, which can help to estimate the approximate size of this candidate PRB.

We use WAC image mosaics and SLDEM2015 data to display the relationship of stratigraphy and lobe morphology for the southwestern region of Orientale Basin. Based on the SLDEM2015 data, we have measured the azimuth radial profiles of elevation by 1° bearing from the north (clockwise, total 360 lines) and computed the average radial profile to determine the diameter of rim–crest and peak–ring. Meanwhile, we measured the depth of this candidate basin. We also produced a hill-shaded map of the research region based on the SLDEM2015 to better highlight the morpho-structural features of the candidate basin. In addition, combining the statistical and empirical formulas (see Formulas (3) and (4) below), we estimated the model initial depth of PRB and the eject thickness from the Orientale basin on this southwest region to explore the evidence or clue for this study. In order to reconstruct the topography of this candidate PRB, we compare the gravity and topography features to a well-preserved peak–ring basin.

3. Results

3.1. GRAIL Bouguer Gravity Anomaly Reconstruction

The Bouguer anomaly (BA) is calculated by removing the separately measured topography. For a typical peak–ring basin, there is usually a large positive BA within a peak–ring and a small or negative anomaly between the peak–ring and the inward edge

of the rim-crest. This is a previously recognized pattern that can help us to recognize the degraded basins that lack apparent rings [13,23,24]. In addition, the correlation between the diameter of the central high Bouguer gravity anomaly and the rim-crest diameter for a well-preserved PRB can aid the identification and characterization of basins for which topographic signatures have been obscured by superposed cratering, ejecta emplacement, or volcanism.

The Bouguer anomaly map of this candidate PRB did have the feature pattern, with central high BA and surrounded by lower BA (Figure 2a). In this study, we firstly determined the center of this candidate PRB according to the maximum Bouguer gravity anomaly in the central area. In addition, the center of this candidate basin is located at 108.8°W, 28.4°S. Secondly, we measured the azimuth radial profiles of Bouguer anomaly by 1° bearing from the north (clockwise, total 360 lines) (Figure 2b) and computed the average radial profile to display the relationship between BA value and basin radius (Figure 2c). The Bouguer anomaly map of the southwestern region of the Orientale basin clearly illustrates a higher central anomaly surrounded by a lower anomaly. The maximum positive Bouguer anomaly ~235 mGal and the minimum value is ~5 mGal (Figure 2c). Following and comparing the locations of the main features of average Bouguer anomaly profiles for PRBs [23], this region has a similar gravity anomaly pattern except the BA value is almost positive (Figure 2a). The lower anomaly annulus extends from the edge of a central positive anomaly and reaches a minimum at approximately midway between the peak-ring and rim-crest. The distance between maximum and minimum value of gravity anomaly is defined as R_{BA} , which has a relationship with the rim-crest radius follows the statistical formula [23]:

$$R_{BA} = 0.74R \pm 0.06R \quad (1)$$

R is the radius of rim-crest and R_{BA} is the distance between the maximum central gravity anomaly and minimum gravity anomaly value.

In this study, the measured R_{BA} value is ~130 km, and calculated the rim-crest radius of this candidate PRB is about 175_{-12}^{+16} km. The Bouguer anomaly contrast of this candidate PRB is about 230 mGal, which is close to the relationship between Bouguer anomaly contrast and main ring diameter [13] (Figure 3).

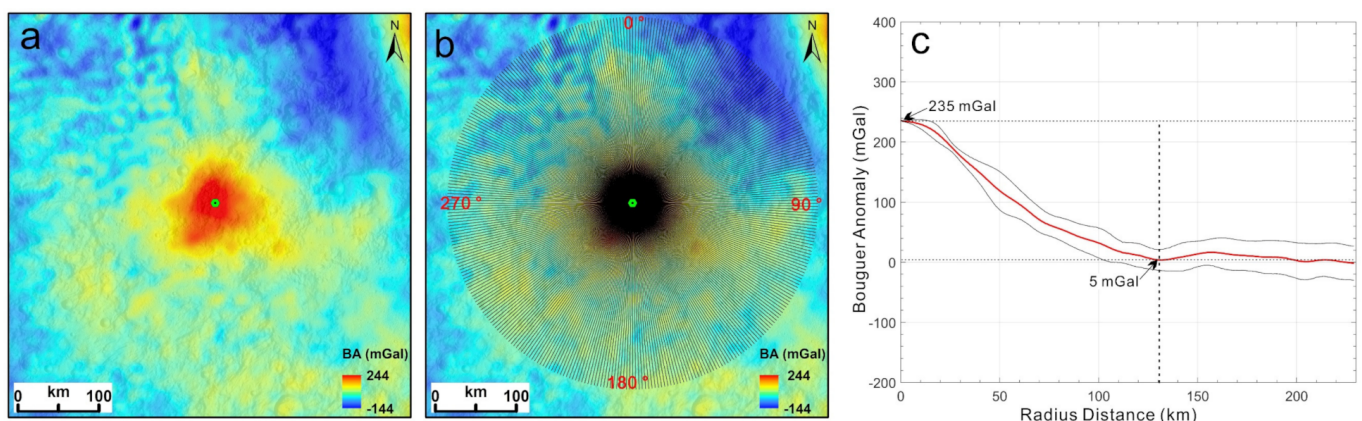


Figure 2. (a) Bouguer anomaly map of the Orientale basin's southwestern region; (b) the azimuth radial profiles of elevation by 1° bearing from the north (clockwise, total 360 lines); (c) the average radial profile (red curve) of Bouguer anomaly and uncertainties (one standard deviation, between the two black curves). The distance between maximum central gravity anomaly and minimum gravity anomaly value (R_{BA}) is ~130 km. (Orthographic Projection centered at 108.8°W, 28.4°S).

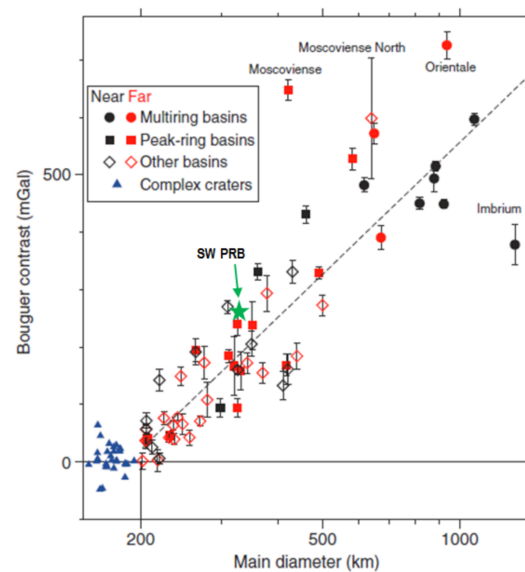


Figure 3. Bouguer anomaly contrast versus main ring diameter (log scale) on the near-side and far-side of the Moon [13]. Open symbols represent possible basins in which multiple rings are not preserved. Green star is the candidate peak–ring basin in southwest of the Orientale basin. The rate of increase in Bouguer anomaly contrast given by a log–linear least squares fit to diameter (dashed line) is about 240 mGal per factor of 2 increase in diameter.

3.2. Topographic Reconstruction of the Original Basin

The degraded pre-Orientale candidate peak–ring basin is adjacent to the Orientale basin to the southwest. Head et al. (2010) recognized the southwestern region as a basin based on the LOLA data superposed on a hillshade rendering of LOLA topography [12]. In this study, based on the center of this candidate PRB that is confirmed by a Bouguer anomaly map, using the SLDEM2015 data, we have measured the azimuth radial profiles of elevation by 1° bearing from the north (clockwise) (Figure 4d).

On the average azimuth radial profile of topography, we determined the location of rim–crest according to the maximum elevation value, and the radius of main rim–crest is ~ 160 km (diameter is ~ 320 km), which is consistent with the result inferred from the Bouguer anomaly map. Along the radial direction to the center of the basin, we determined the location of peak–ring according to the second peak value of elevation, and the radius of peak–ring is ~ 85 km (diameter is ~ 170 km). Meanwhile, we still can identify the remnants of the potential impact structures that can be seen as roughly circular rings after forming the Orientale basin (Figure 4a). Baker et al. (2011) [25] used LOLA data to conduct a survey of craters >50 km in diameter on the Moon, and found a relationship of power-law fit between the peak–ring diameter and rim–crest diameter of peak–ring basins, and the ratio range from 0.35 to 0.56 [25]:

$$D_{ring} = 0.14 \pm 0.10(D_r)^{1.21 \pm 0.13} \quad (2)$$

D_{ring} is the diameter of peak–ring and D_r is the diameter of rim–crest diameter.

For this candidate PRB, the ratio of peak–ring and rim–crest diameter is ~ 0.53 , which is consistent with the statistical result above.

In order to estimate the influence for ejecta emplacement of Orientale basin, we measured the observed depth of this candidate PRB, calculated from the maximum elevation along basin rim to the lowest point on the floor, is about 3.2 km. Meanwhile, we estimated the initial depth after basin formation based on the empirical power law [26]:

$$\log_{10}(d) = 0.41 \times (\log_{10}(D_r))^{0.57} \quad (3)$$

where d is the depth and D_r is the diameter of rim-crest.

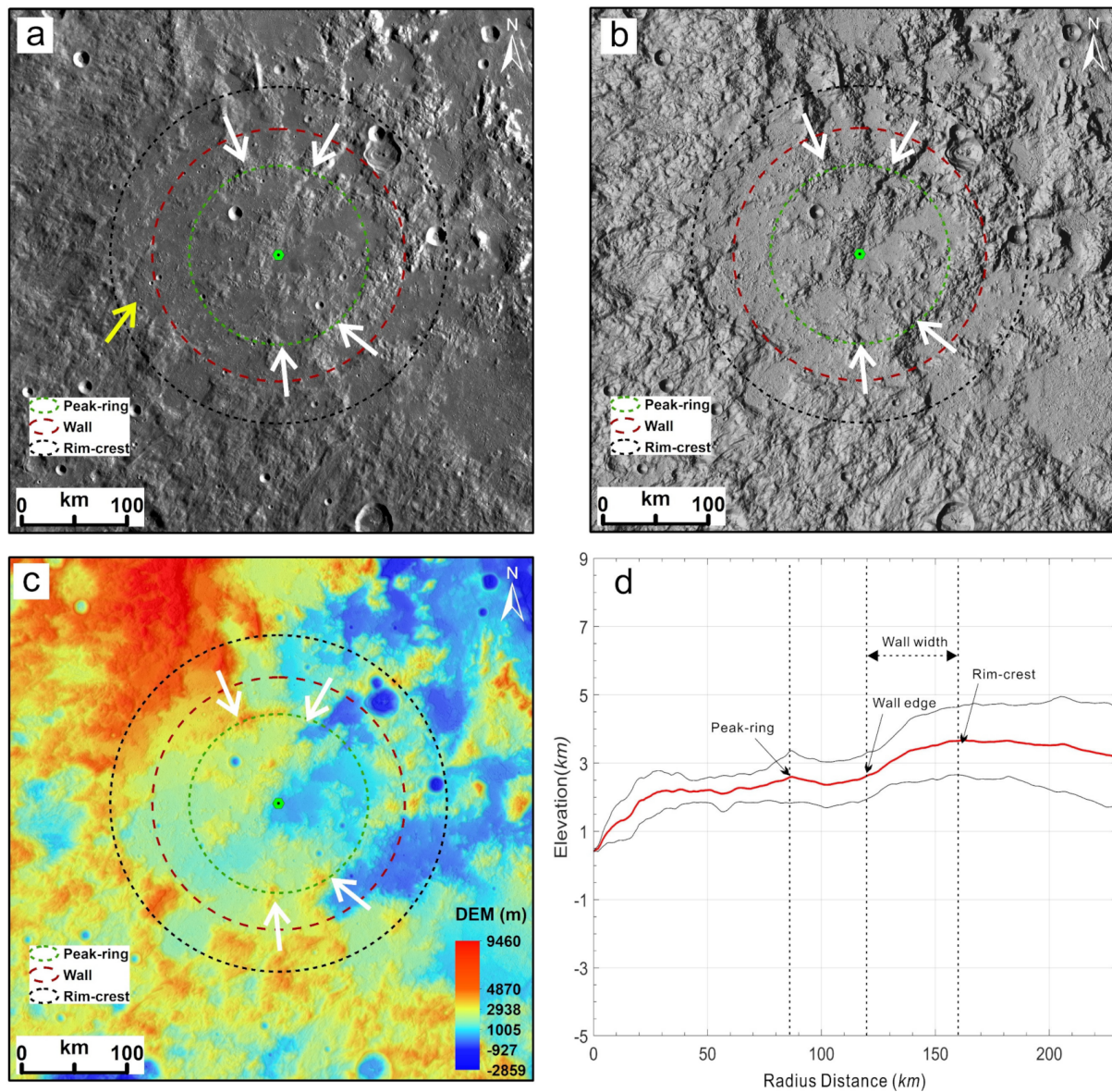


Figure 4. Southwestern region of the Orientale basin: (a) WAC image mosaic; (b) SLDEM2015 hillshade gridded topography; (c) SLDEM2015 colored gridded topography at 59 m/pixel; (d) average azimuth radial profile (red curve) of topography and uncertainties from the averaging are shown as one standard deviation (between the two black curves). The black circle is the rim-crest of the proposed peak-ring basin that is also found in the Bouguer anomaly map (Figure 2), the red circle is the proposed wall, which is the transition zone from the rim to the boundary of the basin floor, the green circle is the proposed peak ring, and the preserved peak-ring was marked by a white arrow and the lobe was marked by a yellow arrow.

The initial depth of this candidate PRB is about 4.90 km, which is larger than observed depth. In this region, the key factor that may be contributing to the smaller depth is the emplacement of ejecta from the Orientale that deposited and superposed on this candidate peak-ring basin. The thickness of ejecta surrounding impact basins on the Moon is approximately modeled by the equation [27]:

$$T = 0.14 \times R^{0.74} \times (r/R)^{-3.0} \quad (4)$$

where T is the thickness of ejecta, r is the range from the center of the basin, and R is the basin radius, and all units are in meters.

For the Orientale basin, the radius is about 465 km (465,000 m), and we estimated the ejecta thickness at the edge of Cordillera ring at about 2190 m, decreasing ~14 m with 1 km distance outside the Cordillera ring, and this result is consistent with the measured result from LOLA data [28]. Following this empirical formula, the ejecta thickness of the Orientale basin, from the center of this peak–ring basin to 160 km (one radius distance) outside of this center, has an estimated range from 0.8–1.8 km, and the ejecta thickness of Orientale basin deposited on the center floor, peak–ring, and rim–crest region are estimated as 1.8 km, 1.1 km, and 0.8 km, respectively. We can infer, before impacting of Orientale and depositing of ejecta, that the initial depth of this candidate peak–ring basin should be 4–5 km with a medium of 4.5 km in depth, which is close to the modeled result (4.9 km).

For an impact basin, the wall is the transition zone from the rim to the edge of the basin floor. Baker et al. (2011) [25] found that wall width decreases from ~30% to ~17% of rim–crest radius from protobasins to the largest peak–ring basins [25]. Based on the average azimuth radial profile of topography, we estimated the wall width is ~40 km, and the radius distance from the basin center is ~120 km. The ratio of the width to the basin radius is ~25%, which is consistent with statistical results.

3.3. Morphologic Reconstruction: Comparison to Schrödinger Peak–Ring Basin

Based on the GRAIL Bouguer gravity anomaly data, we confirmed that this candidate peak–ring basin does exist in the southwestern region of the Orientale basin. However, the initial structure was destroyed by the Orientale impact event or later geological processes. In order to complete reconstruction of this candidate peak–ring basin, we can compare to a similar size peak–ring basin, which is well-preserved. On the Moon, the Schrödinger peak–ring basin, located on the lunar far-side and within the oldest South Pole–Aitken basin (centered at 132.9°E, 74.7°S), is one of the least modified lunar peak–ring basins with a well-preserved gravity anomaly feature and morphological structure [5,29–32].

In this study, we first compared the Bouguer gravity anomaly characteristics of the candidate PRB and Schrödinger PRB, and they have a similar feature pattern with central high BA and are surrounded by lower BA (Figure 5a,b). We also measured the azimuth radial profiles of Bouguer anomaly by 1° bearing from the north (clockwise, total 360 lines) for the Schrödinger peak–ring basin, and, compared to this candidate PRB, they have a similar trend from the basin center to the edge of PRB, except the BA value (Figure 5c). In addition, the R_{BA} of Schrödinger PRB is about 140 km, which is close to R_{BA} of this candidate PRB (R_{BA} is about 130 km), indicating that they are relatively close in size.

Secondly, we compared the topographic features of the two basins. For this candidate PRB, the topography has been destroyed and only existed remnants of the potential ring structures (Figure 5d). However, for Schrödinger PRB, the rim–crest is well-preserved and approximately circular, and the inner peak–ring is represented by a discontinuous ring of mountains (Figure 5e). In this study, we also measured the azimuth radial profiles of elevation by 1° bearing from the north (clockwise, total 360 lines) for Schrödinger PRB and, compared to this candidate PRB (Figure 5f), with the similar trend of from the basin center to the edge of PRB, except the elevation value. The rim–crest and peak–ring’s diameters of Schrödinger PRB are ~325 km and ~166 km, respectively. Similarly, the rim–crest and peak–ring’s diameter of this candidate PRB are ~320 km and ~170 km, respectively. It is worth noting that the average observed depths of the two PRBs are obviously different. The average observed depth of Schrödinger PRB is about 4.2 km, while this candidate PRB’s average observed depth is only about 3.2 km. In addition, we estimated that the ejecta thickness of the Orientale basin on this candidate PRB region has a range from 0.8–1.8 km (Section 3.2, Formula (4)). Considering the influence of the deposited ejecta from the Orientale basin, if we remove the eject thickness, the depth of this candidate PRB ranges from 4.0–5.0 km, which is similar to the average observed depth of Schrödinger PRB.

Through the above comparison and analysis, we further confirmed that this candidate PRB is a pre-existing PRB before the Orientale impact event. Both two PRBs are very close in size, and the Schrödinger basin can be a good example for a comparison and

reference to reconstruct the modified candidate peak–ring basin in this study (Figure 5). The relative fresh morphologic structure of the candidate peak–ring basin should be similar to Schrödinger PRB, with a well-preserved circular rim–crest and inner peak–ring. However, the current topography is destroyed by formation of the Orientale basin’s rings, which are disturbed by this pre-existing negative topography in the meantime.

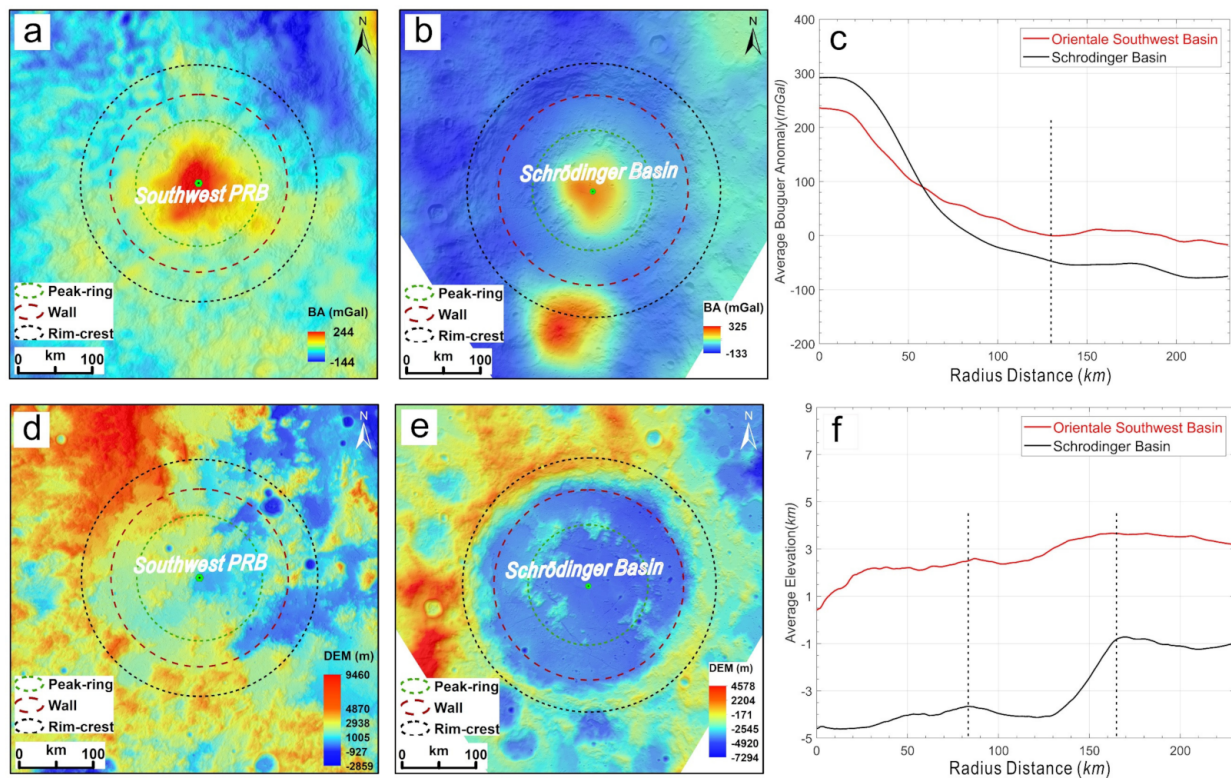


Figure 5. Comparison between pre-Oriente southwest peak–ring basin (left panel) and Schrödinger peak–ring basin (middle panel): Bouguer anomaly (up, a–c), Topography (down, d–f). (a,d: Orthographic Projection centered at 108.8°W, 28.4°S; b,e: Orthographic Projection centered at 132.9°E, 74.7°S).

4. Discussion

The surface of the moon is almost completely full of impact craters and basins. For degraded basins, it is difficult to recognize from the topography feature. The Bouguer anomaly (BA) is calculated by removing the separately measured topography, which retains the deep structural features of the impact basin, such as substantial mantle uplifts. For a typical peak–ring basin, the identified Bouguer anomaly pattern is usually a large positive BA within the peak–ring and surrounded by lower BA, which can be used to recognize the degraded basins that lack apparent rings [13,23,24]. In addition, the empirical relationship between the diameter of the central high Bouguer gravity anomaly and the rim–crest diameter for a well-preserved PRB can aid the identification and characterization of basins for which topographic signatures have been obscured by superposed cratering, ejecta emplacement, or volcanism formula [23]. Combining the high-resolution topography data and empirical formulas, we can recognize the remnant ring structure, which provides additional evidence to confirm a degraded or buried basin on the Moon. In addition, we can reconstruct the relative initial topography of a degraded basin by comparing and referencing a typical and young basin with a similar size, which can provide plenty of clues or evidence for reconstruction.

At the southwestern region of the Orientale basin, the massifs most extensively developed where ring structures are difficult to distinguish, and the previous geologic map showed an outward extension of Cordillera ring [3,4,6,7]. Our study confirms previous interpretations that a large pre-Oriente peak–ring basin is located southwest of the Ori-

entale basin. The remnants of this potential PRB ring structures can be seen as roughly circular features of high topography encircling a lower topography (Figure 4). This candidate PRB's average observed depth is only about 3.2 km. In addition, we estimated that the ejecta thickness of the Orientale basin on this candidate PRB region ranges from 0.8–1.8 km (Section 3.2, Formula (4)). Considering the influence of the deposited ejecta from the Orientale basin, if we remove the ejecta thickness, the depth of this candidate PRB ranges from 4.0–5.0 km, which is close to the modeled result (4.9 km) and similar to the average observed depth of Schrödinger PRB. The presence of pre-existing PRB structures disrupted the coherent formation of the Cordillera ring, which cuts and crosses the PRB in the meantime. In addition, the edge of this PRB is close to the edge of the Outer Rook ring, which was also interrupted by this pre-existing PRB and contributed to the complexity of this region with a wide and discontinuous massif. When taking these topographic features into consideration, we suggest that the Cordillera ring would be more complete and more continuous across this southwestern region with a distinct low topography space, similar to the rest of the Orientale basin with nearly circular rings. Thus, we can also infer that the Cordillera ring is a quasi-circumferential and semi-continuous distinctive scarp [14] through the center of this southwestern PRB; in addition, the Outer Rook ring formed at the edge of this PRB.

Due to the pre-existence of the negative-relief topographic structures, the portion of ejecta flow material from Orientale around this region should have overcome this topographic obstacle, such as rim and peak–ring of this PRB, and then collected in the low interiors, which is the main reason that the smooth member of the Montes Rook Formation is mainly concentrated in the southwestern quadrant of the basin interior with minor extensions beyond the Cordillera basin rim crest [7]. A flow lobe was also seen at this extension region (Figure 4a), suggesting some type of fluid movement of material during the late stages of emplacement and deposited there. Furthermore, the location and preservation of the peak–ring basin Bouguer anomaly strongly suggest that the rim crest of the Orientale basin excavation cavity lies at or within the Outer Rook Mountain ring.

5. Conclusions

The southwestern region of the Orientale basin is topographically complex, where the Cordillera ring is an outward excursion of ring structures and the Outer Rook ring is likewise distorted with wider ring massifs. The occurrence of a highly degraded pre-Orientale peak–ring basin (PRB) adjacent to the Orientale basin to the southwest could be an important key to address these questions. In this study, based on multiple datasets, including the GRAIL Bouguer gravity anomaly, SLDEM2015, and WAC mosaic images, combining the statistical and empirical formulas [13,23,25–27], we confirmed that the southwestern region of Orientale basin is a pre-existing peak–ring basin, whose center is 108.8°W, 28.4°S with ~320 km rim–crest diameter and ~170 km peak–ring diameter. In addition, we compared this candidate PRB to the Schrödinger PRB to reconstruct the topography of this Pre-Orientale southwest PRB. This candidate PRB's average observed depth is only about 3.2 km. Considering the influence of the deposited ejecta from the Orientale basin, if we remove the ejecta thickness, the depth of this candidate PRB ranges from 4.0–5.0 km, which is close to the modeled result (4.9 km) and similar to the average observed depth of Schrödinger PRB. The pre-Orientale peak–ring basin, negative-relief topographic structures, disrupted the coherent development of the Cordillera ring and emplacement of ejecta when forming the Orientale basin, which is the reason that the smooth member of the Montes Rook Formation is mainly concentrated in the southwestern region. Without the presence of this pre-existing peak–ring basin, the Cordillera would be more complete and more contiguous through this southwestern section, which would be more similar to the rest of the Orientale basin that has close to circular rings.

Author Contributions: All authors made significant contributions to the work. J.J.: methodology, investigation, writing—original draft preparation; J.W.H.: conceptualization, formal analysis, investi-

gation, writing—review & editing; J.L.: conceptualization, investigation, writing—review & editing, funding acquisition. All authors have read and agreed to the published version of the manuscript.

Funding: This research was funded by the Strategic Priority Research Program of Chinese Academy of Sciences (grant number, XDB 41000000), the National Natural Science Foundation of China (grant number, 41773065), the Key Research Program of Frontier Sciences CAS (grant number, QYZDY-SSW-DQC028) and the Natural Science Foundation of Inner Mongolia, China (grant number, 2020LH04002).

Data Availability Statement: The study did not report any data.

Acknowledgments: The authors would like to thank the editor and reviewers for constructive reviews and comments that helped improve the manuscript. We gratefully acknowledge the, LROC, SLDEM2015 and GRAIL teams for their efforts in obtaining and processing the data that went into this work.

Conflicts of Interest: The authors declare no conflict of interest.

References

- Hartmann, W.K.; Wood, C.A. Moon: Origin and evolution of multi-ring basins. *Moon* **1971**, *3*, 3–78. [[CrossRef](#)]
- Head, J.W. Orientale multi-ringed basin interior and implications for the petrogenesis of lunar highland samples. *Moon* **1974**, *11*, 327–356. [[CrossRef](#)]
- McCauley, J.F. Orientale and Caloris. *Phys. Earth Planet. Inter.* **1977**, *15*, 220–250. [[CrossRef](#)]
- Moore, H.; Hodges, C.; Scott, D. Multiringed basins—illustrated by Orientale and associated features. *Lunar Planet. Sci. Conf. Proc.* **1974**, *5*, 71–100.
- Wilhelms, D.E.; McCauley, J.F.; Trask, N.J. *The Geologic History of the Moon*; US Government Printing Office: Washington, DC, USA; Denver, CO, USA, 1987.
- Scott, D.H.; McCauley, J.F. *Geologic Map of the West Side of the Moon*; US Geological Survey; Citeseer: Reston, VA, USA, 1977.
- Spudis, P.D.; Martin, D.J.P.; Kramer, G. Geology and composition of the Orientale Basin impact melt sheet. *J. Geophys. Res. Planets* **2014**, *119*, 19–29. [[CrossRef](#)]
- Schultz, P.H.; Spudis, P.A. The Dark Ring of Orientale: Implications for Pre-Basin Mare Volcanism and a clue to the identification of the transient cavity rim. In Proceedings of the Lunar Planetary Science Conference, Houston, TX, USA, 13–17 March 1978; Volume 9, pp. 1033–1035.
- Spudis, P. Multi-ring basins and planetary evolution. In *The Geology of Multi-Ring Impact Basins: The Moon and Other Planets (Cambridge Planetary Science Old)*; Cambridge University Press: Cambridge, UK, 1993; pp. 224–231.
- Wood, C.A.; Collins, M.J.S. New light on old basins. In Proceedings of the Lunar Planetary Science Conference, The Woodlands, TX, USA, 7–11 March 2011; Volume 1608, p. 1314.
- Solomon, S.C.; Head, J.W. Lunar Mascon Basins: Lava Filling, Tectonics, and Evolution of the Lithosphere. *Rev. Geophys. Space Phys.* **1980**, *18*, 107–141. [[CrossRef](#)]
- Head, J.W.; Fassett, C.I.; Kadish, S.J.; Smith, D.E.; Zuber, M.T.; Neumann, G.A.; Mazarico, E. Global distribution of large lunar craters: Implications for resurfacing and impactor populations. *Science* **2010**, *329*, 1504–1507. [[CrossRef](#)]
- Neumann, G.A.; Zuber, M.T.; Wieczorek, M.A.; Head, J.W.; Baker, D.M.; Solomon, S.C.; Smith, D.E.; Lemoine, F.G.; Mazarico, E.; Sabaka, T.J. Lunar impact basins revealed by Gravity Recovery and Interior Laboratory measurements. *Sci. Adv.* **2015**, *1*, e1500852. [[CrossRef](#)]
- Morse, Z.R.; Osinski, G.R.; Tornabene, L.L. New morphological mapping and interpretation of ejecta deposits from Orientale Basin on the Moon. *Icarus* **2018**, *299* (Suppl. C), 253–271. [[CrossRef](#)]
- Robinson, M.S.; Brylow, S.M.; Tschimmel, M.; Humm, D.; Lawrence, S.J.; Thomas, P.C.; Denevi, B.; Bowman-Cisneros, E.; Zerr, J.; Ravine, M.A.; et al. Lunar reconnaissance orbiter camera (LROC) instrument overview. *Space Sci. Rev.* **2010**, *150*, 81–124. [[CrossRef](#)]
- Zuber, M.T.; Smith, D.E.; Watkins, M.M.; Asmar, S.W.; Konopliv, A.S.; Lemoine, F.G.; Melosh, H.J.; Neumann, G.A.; Phillips, R.J.; Solomon, S.C.; et al. Gravity Field of the Moon from the Gravity Recovery and Interior Laboratory (GRAIL) Mission. *Science* **2013**, *339*, 668. [[CrossRef](#)]
- Lemoine, F.G.; Goossens, S.; Sabaka, T.J.; Nicholas, J.B.; Mazarico, E.; Rowlands, D.D.; Loomis, B.; Chinn, D.S.; Caprette, D.S.; Neumann, G.A.; et al. High degree gravity models from GRAIL primary mission data. *J. Geophys. Res. Planets* **2013**, *118*, 1676–1698. [[CrossRef](#)]
- Goossens, S.; Lemoine, F.G.; Sabaka, T.J.; Nicholas, J.B.; Mazarico, E.; Rowlands, D.D.; Loomis, B.D.; Chinn, D.S.; Neumann, G.A.; Smith, D.E.; et al. A Global Degree and Order 1200 Model of the Lunar Gravity Field Using GRAIL Mission Data. In Proceedings of the Lunar Planetary Science Conference, The Woodlands, TX, USA, 21–25 March 2016; Volume 1903, p. 1484.
- Barker, M.; Mazarico, E.; Neumann, G.; Zuber, M.; Haruyama, J.; Smith, D. A new lunar digital elevation model from the Lunar Orbiter Laser Altimeter and SELENE Terrain Camera. *Icarus* **2016**, *273*, 346–355. [[CrossRef](#)]

20. Konopliv, A.S.; Park, R.S.; Yuan, D.N.; Asmar, S.W.; Watkins, M.M.; Williams, J.G.; Fahnestock, E.; Kruizinga, G.; Paik, M.; Strelakov, D.; et al. High-resolution lunar gravity fields from the GRAIL Primary and Extended Missions. *Geophys. Res. Lett.* **2014**, *41*, 1452–1458. [[CrossRef](#)]
21. Lemoine, F.G.; Goossens, S.; Sabaka, T.J.; Nicholas, J.B.; Mazarico, E.; Rowlands, D.D.; Loomis, B.D.; Chinn, D.S.; Neumann, G.A.; Smith, D.E.; et al. GRGM900C: A degree 900 lunar gravity model from GRAIL primary and extended mission data. *Geophys. Res. Lett.* **2014**, *41*, 3382–3389. [[CrossRef](#)]
22. Evans, A.J.; Soderblom, J.M.; Andrews-Hanna, J.C.; Solomon, S.C.; Zuber, M.T. Identification of buried lunar impact craters from GRAIL data and implications for the nearside maria. *Geophys. Res. Lett.* **2016**, *43*, 2445–2455. [[CrossRef](#)]
23. Baker, D.M.H.; Head, J.W.; Phillips, R.R.J.; Neumann, G.A.; Bierson, C.J.; Smith, D.E.; Zuber, M.T. GRAIL gravity observations of the transition from complex crater to peak-ring basin on the Moon: Implications for crustal structure and impact basin formation. *Icarus* **2017**, *292*, 54–73. [[CrossRef](#)]
24. Byrne, C.J. *The Moon's Largest Craters and Basins*; Springer International Publishing: Berlin/Heidelberg, Germany, 2016.
25. Baker, D.M.H.; Head, J.W.; Fassett, C.I.; Kadish, S.J.; Smith, D.E.; Zuber, M.T.; Neumann, G.A. The transition from complex crater to peak-ring basin on the Moon: New observations from the Lunar Orbiter Laser Altimeter (LOLA) instrument. *Icarus* **2011**, *214*, 377–393. [[CrossRef](#)]
26. Williams, K.K.; Zuber, M.T. Measurement and analysis of lunar basin depths from Clementine altimetry. *Icarus* **1998**, *131*, 107–122. [[CrossRef](#)]
27. McGetchin, T.R.; Settle, M.; Head, J.W. Radial thickness variation in impact crater ejecta: Implications for lunar basin deposits. *Earth Planet. Sci. Lett.* **1973**, *20*, 226–236. [[CrossRef](#)]
28. Fassett, C.I.; Head, J.W.; Smith, D.E.; Zuber, M.T.; Neumann, G.A. Thickness of proximal ejecta from the Orientale Basin from Lunar Orbiter Laser Altimeter (LOLA) data: Implications for multi-ring basin formation. *Geophys. Res. Lett.* **2011**, *38*, L17201. [[CrossRef](#)]
29. Mest, S.C. The geology of Schrödinger basin: Insights from post-Lunar Orbiter data. In *Recent Advances and Current Research Issues in Lunar Stratigraphy*; Ambrose, W.A., Williams, D.A., Eds.; Geological Society of America: Boulder, CO, USA, 2011.
30. Kramer, G.Y.; Kring, D.A.; Nahm, A.L.; Pieters, C.M. Spectral and photogeologic mapping of Schrödinger Basin and implications for post-South Pole-Aitken impact deep subsurface stratigraphy. *Icarus* **2013**, *223*, 131–148. [[CrossRef](#)]
31. Xu, L.; Xie, M. Ejecta thickness distribution of the Schrödinger Basin on the Moon. *J. Geophys. Res. Planets* **2020**, *125*, e2020JE006506. [[CrossRef](#)]
32. Czaplinski, E.C.; Harrington, E.M.; Bell, S.K.; Tolometti, G.D.; Farrant, B.E.; Bickel, V.T.; Kring, D.A. Human-assisted Sample Return Mission at the Schrödinger Basin, Lunar Far Side, Using a New Geologic Map and Rover Traverses. *Planet. Sci. J.* **2021**, *2*, 51. [[CrossRef](#)]